

Hydraulic performance testing of a concrete mattress

By L Montano and B M Miller

WRL TR 2020/40, December 2020



UNSW
Water Research
Laboratory



UNSW
SYDNEY



Water
Research
Laboratory
School of Civil and
Environmental Engineering

Hydraulic Performance Testing of a Concrete Mattress

WRL TR 2020/40 December 2020

By L Montano and B M Miller

Project details

Report title	Hydraulic Performance Testing of a Concrete Mattress
Authors(s)	L Montano and B M Miller
Report no.	2020/40
Report status	Final
Date of issue	
WRL project no.	2019063
Project manager	B Miller
Client	Australian Concrete Mats
Client address	Alstonville NSW 2477
Client contact	Richard Mould info@concretemats.com.au
Client reference	#

Document status

Version	Reviewed by	Approved by	Date issued
Draft	S Felder	G P Smith	03 December 2020
Final	G P Smith	G P Smith	11 December 2020



**Water
Research
Laboratory**
School of Civil and
Environmental Engineering

www.wrl.unsw.edu.au

110 King St, Manly Vale, NSW, 2093, Australia
Tel +61 (2) 8071 9800, ABN 57 195 873 179



This report was produced by the Water Research Laboratory, School of Civil and Environmental Engineering, University of New South Wales Sydney for use by the client in accordance with the terms of the contract.

Information published in this report is available for release only with the permission of the Director, Water Research Laboratory and the client. It is the responsibility of the reader to verify the currency of the version number of this report. All subsequent releases will be made directly to the client.

The Water Research Laboratory shall not assume any responsibility or liability whatsoever to any third party arising out of any use or reliance on the content of this report.

Contents

1	Summary of Findings	1
2	Measurement Methods	5
2.1	Experimental configuration	5
3	Visual observations	9
4	Measurements	18
4.1	Flow depth	18
4.2	Depth averaged velocity	20
4.3	Shear stress	21
4.4	Darcy friction factor	22
4.5	Manning coefficient	24
5	Example of calculating uniform flow depth and velocity for the concrete mats	26
6	References	29
Appendix A Instrumentation		
Appendix B Uniform flow conditions		

List of tables

Table 1-1 Summary of hydraulic parameters for tests with and without the concrete mattress	3
Table 3-1 Aeration and flow elevation comparison for experiments conducted with and without the concrete mat at the channel downstream (note that the photos have been rotated)	9
Table 3-2 Free-surface roughness comparison for tests conducted with and without the concrete mat	11
Table 3-3 Aeration comparison for tests conducted with and without the concrete mat	15

List of figures

Figure 1-1 Test facility	1
Figure 1-2 Dimensions and appearance of concrete blocks in the mattress	1
Figure 1-3 Comparison of flows in the artificial turf (top) channel and concrete mattress channel (bottom)	2
Figure 2-1 WRL spillway flume	5
Figure 2-2 Channel bed configurations in the spillway flume	6
Figure 2-3 Transverse measurement locations in the concrete mattress setup	7
Figure 2-4 Sketch of the experimental configuration for the analysis of hydraulic performance of the concrete mats (not to scale)	8
Figure 4-1 Definition of artificial turf flow depth elevation	18
Figure 4-2 Definition of concrete flow depth elevations	19
Figure 4-3 Comparison uniform flow depths	20
Figure 4-4 Comparison of mean velocity considering discharges without and with concrete mattress	21
Figure 4-5 Comparison of mean shear stress considering discharges without and with concrete mattress	22
Figure 4-6 Comparison of Darcy friction factors	23
Figure 4-7 Darcy friction factor as a function of the flow depth	24
Figure 4-8 Manning's "n" coefficient for concrete mats	25
Figure 5-1 Darcy friction factor for the concrete mat as a function of the flow depth	26
Figure 5-2 Flow chart for estimating uniform flow depths and mean flow velocities for open channels with concrete mats	28
Figure A-1 Brook Crompton centrifugal pump	30
Figure A-2 Ultrasonic arrangement in the channel centre line	30
Figure B-1 Uniform flow conditions in channel centre line at the downstream end of the flume	32

1 Summary of Findings

Australian Concrete Mats (www.concretemats.com.au) engaged the UNSW Water Research Laboratory (WRL) to undertake laboratory testing of a flexible concrete mattress to determine the hydraulic roughness properties and the bed shear under a range of flowrates.

The mattress was tested in WRL's spillway flume as shown in Figure 1-1. The mattress was composed of rough concrete blocks with an approximate size of 160 mm x 148 mm x 58 mm high, attached to a polyester geogrid to provide a regular 40 mm spacing between each block. The dimensions and appearance of the mattress blocks are shown in Figure 1-2.



Figure 1-1 Test facility

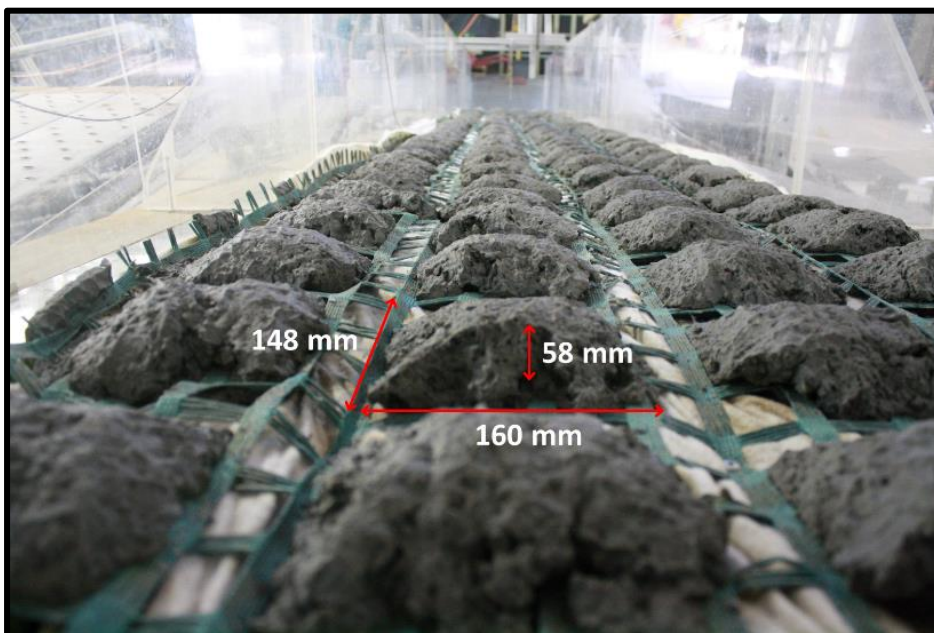


Figure 1-2 Dimensions and appearance of concrete blocks in the mattress

The scope of testing included one slope of 11 degrees representing typical moderate slopes of embankments. The flume was 9 m long and the reported flow depths were measured at the downstream end of the flume after uniform flow had been achieved. The flume was 0.8 m wide and all flowrates are reported as flow per metre width ($\text{m}^3/\text{s}/\text{m}$).

Tests were also undertaken without the concrete mattress but with an artificial turf to represent the bed conditions of an unlined channel to provide a comparison of the flow conditions.

The concrete mattress provided “macro-roughness” to the channel. Flows over the concrete mattress resulted in bubbly, aerated flow with a significant increase in flow depth (approximately 1.5 times) and a substantial decrease in depth averaged flow velocity (between 30 to 60%) when compared to flow over the artificial turf (unlined channel). Visual comparison of the flows at $0.25 \text{ m}^3/\text{s}/\text{m}$ are shown in Figure 1-3.



Figure 1-3 Comparison of flows in the artificial turf (top) channel and concrete mattress channel (bottom)

Further visual observations and photographs are presented in Section 3 of this report.

Measured hydraulic parameters both with and without the concrete mattress are presented in Table 1-1. Further details are included in Section 4.

Table 1-1 Summary of hydraulic parameters for tests with and without the concrete mattress

Test		Flow rate per unit of width (m ³ /s/m)	Depth (m)	Velocity (m/s)	Darcy friction factor <i>f</i>	Manning coefficient <i>n</i>
Concrete mattress	Artificial turf					
X		0.06	0.08	0.71	2.42	0.12
X		0.125	0.10	1.20	1.10	0.08
X		0.188	0.12	1.53	0.80	0.07
X		0.250	0.14	1.83	0.63	0.06
X		0.375	0.16	2.34	0.45	0.06
	X	0.06	0.03	1.95	0.13	0.02
	X	0.125	0.05	2.61	0.10	0.01
	X	0.188	0.06	3.15	0.09	0.01
	X	0.250	0.07	3.54	0.08	0.01
	X	0.375	0.09	4.12	0.08	0.01

The flow depths presented in Table 1-1 correspond to the centreline of the channel. Note that for the lowest flowrate, the flow depth in the middle of the channel (between the blocks) was lower than where the flow had to pass over the concrete blocks. The flow regime was supercritical for cases other than the lowest flowrate. The estimation of the hydraulic parameters was conducted as indicated below:

- Flow depths were measured using methods described in Appendix A .
- Velocity was calculated as the depth averaged velocity.
- The Darcy friction factor (*f*) was calculated based on Equation 1.

$$V = \sqrt{\frac{8 \cdot g \cdot R_h \cdot S_0}{f}} \quad \text{Equation 1}$$

- The Manning friction factor (*n*) was calculated based on Equation 2.

$$V = \frac{1}{n} \cdot R_h^{\left(\frac{2}{3}\right)} \cdot S_0^{\left(\frac{1}{2}\right)} \quad \text{Equation 2}$$

In all of the tests the hydraulic radius (R_h) can be approximated as the flow depth (d) because the flow was relatively shallow when compared to the channel width (b), i.e. $b/d \geq 4$, and because the walls of the flume were relatively smooth compared to the bed.

Details of the measurement and calculation methods are presented in Section 2 and Appendix A . Graphs detailing the relationship between flow rate and the various friction factors are provided in Section 4 with an example for estimating the flow depth based on the friction factor in Section 5.

The results presented in this document are limited to:

- A concrete mat of 58 mm height, a block size area of 160 mm x 148 mm with the same grid pattern as presented in Figure 1-2.
- Discharges between 0.06 m³/s/m to 0.4 m³/s/m.
- Uniform flow conditions.
- Slopes up to 11 degrees

The concrete mattress was observed to be stable for the range of velocities tested (0.7 m/s to 2.3 m/s) suggesting that the mattress was stable at velocities up to 2.3 m/s. The mattress may tolerate larger velocities, but further tests with larger velocities would be required.

Based on the observed flow patterns, it is highly recommended that another laterally offset block distribution pattern is considered to increase flow disturbance and so avoid flow channelling between the blocks.

2 Measurement Methods

2.1 Experimental configuration

The experiments were conducted in the spillway flume of the UNSW's Water Research Laboratory (Figure 2-1). The spillway flume was 0.8 m wide and 9 m long and had a slope of 11 degrees representing typical moderate slopes of embankments.



Figure 2-1 WRL spillway flume

The base flow conditions considered an artificial turf to represent the bed conditions of an unlined channel (Figure 2-2a). Note the artificial turf does not include roots and soil and therefore, the roughness of this artificial turf is lower than expected for real grass channels. Identical flow conditions were repeated with the Australian Concrete Mattress anchored to the channel (Figure 2-2b).



(a) Artificial turf



(b) Concrete mat

Figure 2-2 Channel bed configurations in the spillway flume

During concrete mattress testing, measurements were taken at two (2) locations across the width of the flume (transverse cross-section):

- Channel centre line measurements between the concrete blocks; and
- the top of the concrete blocks at a distance of 0.10 m from the centre line measurements (Figure 2-3).

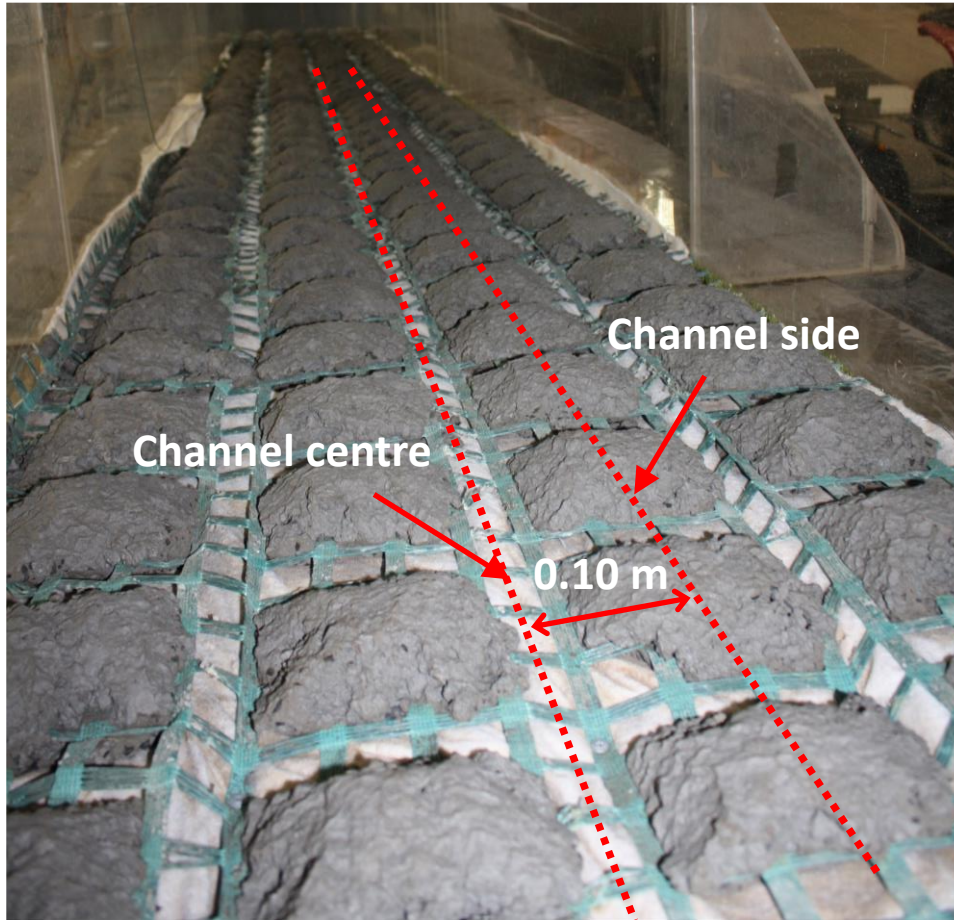


Figure 2-3 Transverse measurement locations in the concrete mattress setup

Figure 2-4 shows the experimental configuration with concrete mattress and the instrumentation used. Visual observations were recorded for flows between $0.03 \text{ m}^3/\text{s}/\text{m}$ to $0.375 \text{ m}^3/\text{s}/\text{m}$ and flow depth measurements were obtained over a range of $0.06 \text{ m}^3/\text{s}/\text{m}$ to $0.375 \text{ m}^3/\text{s}/\text{m}$.

As the flow travels over the mats, air is entrained into the flow. The air entrainment starts at the inception point of free-surface aeration and uniform flow is achieved after a certain distance at the region where the flow depth and air concentration is constant (Appendix B). The flow depths were recorded at four (4) locations down the flume between 7.00 m to 7.75 m to ensure that results represent uniform flow conditions.

Flow rates were measured with a calibrated electromagnetic flow meter. For non-aerated flows, time-averaged flow depths were recorded with four ultrasonic sensors located along the centreline of the channel, sampled for three (3) minutes at a frequency of 100 Hz. The time-averaged flow depths of the aerated flows were determined using a double-tip conductivity probe and compared with the ultrasonic sensor measurements. Conductivity probes have been widely used in the analysis of complex air-water flows (Chanson and Toombes 2002; Felder and Pfister 2017; Scheres et al. 2019). The conductivity probe was mounted on a robotic arm allowing the recording at different elevations. The conductivity probe measurements were undertaken for 45 seconds at a frequency of 20 kHz as recommended by Felder and Chanson (2015) at the channel centre line and at the channel side line. Detailed information of all instrumentation and data processing is included in Appendix A.

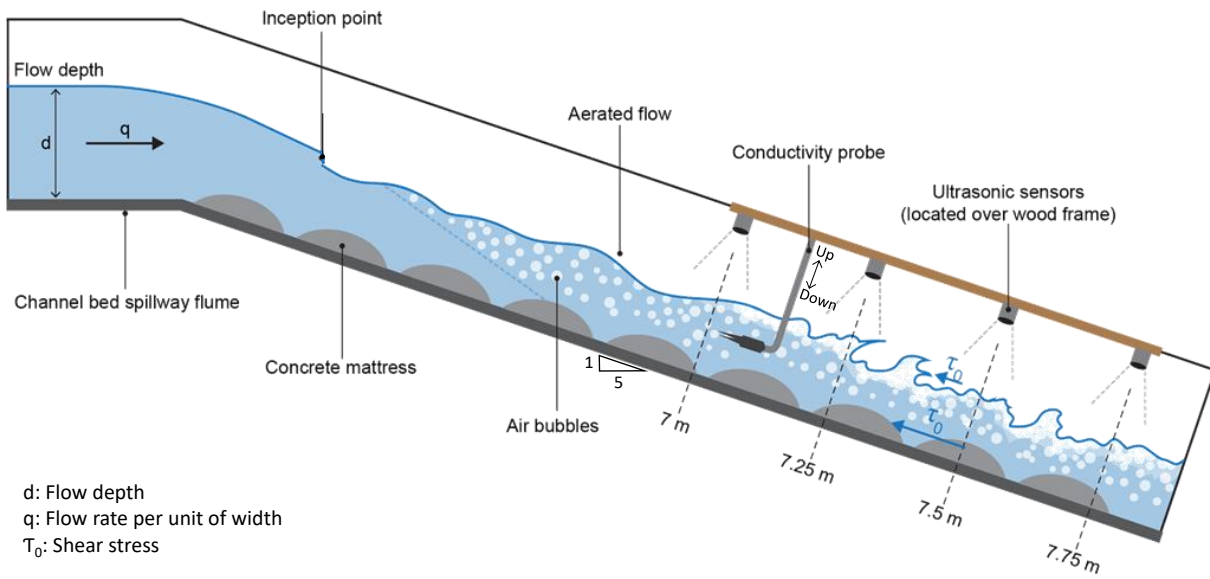


Figure 2-4 Sketch of the experimental configuration for the analysis of hydraulic performance of the concrete mats (not to scale)

3 Visual observations

This chapter presents a visual comparison of the flow features between the experiments conducted with the artificial turf and the concrete mat for a range of flow rates. Overall, significant differences were observed in the aeration, flow depths and free-surface roughness. Table 3-1 presents the visual comparison in the aeration and flow elevation between the flows with the artificial turf and the concrete mat at the downstream end of the channel in the uniform flow region. The main differences were:

- The flow depth was considerably higher and presented larger free-surface fluctuations for the concrete mattress tests.
- Water splashes and droplets were continuously observed for the concrete mat tests while a smoother and more uniform free-surface elevation was identified in the artificial turf tests.
- Localised hydraulic jumps were observed between each concrete block for flows lower than $0.06 \text{ m}^3/\text{s}/\text{m}$ resulting in larger water surface variability.
- Aeration was consistently observed for the concrete mattress tests due to large roughness and breaking of the free-surface.
- Concrete mats were observed to lift and move slightly for flows of $0.188 \text{ m}^3/\text{s}/\text{m}$ or greater in areas where the mat was not anchored to the channel bed.

Table 3-1 Aeration and flow elevation comparison for experiments conducted with and without the concrete mat at the channel downstream (note that the photos have been rotated)

$q \text{ (m}^3/\text{s}/\text{m)}$	Artificial turf	Concrete Mat
0.03		
0.06		
0.125		


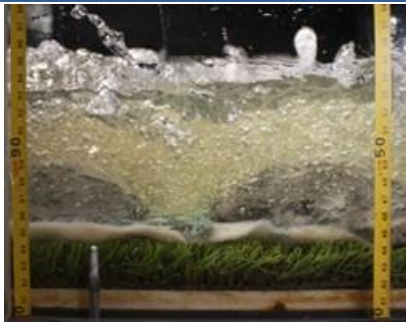





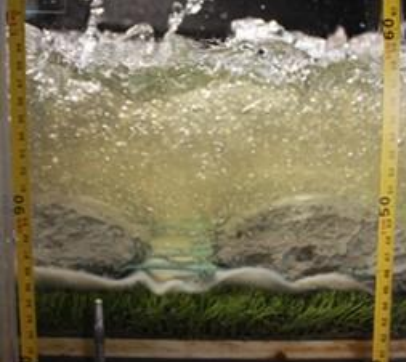
q (m ³ /s/m)	Artificial turf	Concrete Mat
0.188		
0.250		
0.313		
0.375		

Table 3-2 and Table 3-3 present a comparison between the artificial turf and concrete mattress experiments in the free-surface roughness development along the flume. The main differences in the surface roughness between the experiments conducted with the artificial turf and the concrete mat are summarised below:

- For both conditions, the channel bed roughness generated free-surface disturbances along the flume and these disturbances increased with increasing the flow rate. For the concrete mat tests, the free-surface was more fragmented, whitish and was characterised by strong air entrainment and entrapment.
- Minor flow aeration was observed along the flume for the artificial turf tests, whereas the concrete mat tests had large flow aeration for all flow rates investigated.

- The free-surface roughness was similar across the channel width for the tests conducted with the artificial turf for all flow rates. For the concrete mat tests and for flows lower than 0.06 m³/s/m, transverse variations in the free-surface were observed. In the channel side line, hydraulic jumps were identified downstream of each concrete block resulting in higher flow depths on top of the concrete blocks. In the channel centre line, the intermediate area between the blocks performed as a channel resulting in lower flow depths and faster flows.
- For concrete mat tests conducted with large flows (flows above 0.188 m³/s/m), strong instabilities were observed along the flume but minor transverse differences were visually identified. This is linked with the larger submergence of the concrete blocks for higher flow depths.
- The inception point distance, representing the initial location of free-surface aeration along the flume, was shorter in the tests conducted with the concrete mattress as can be observed in Table 3-2 and Table 3-3.

Table 3-2 Free-surface roughness comparison for tests conducted with and without the concrete mat

q (m ³ /s/m)	Artificial turf	Concrete Mat
0.03		

q (m³/s/m)

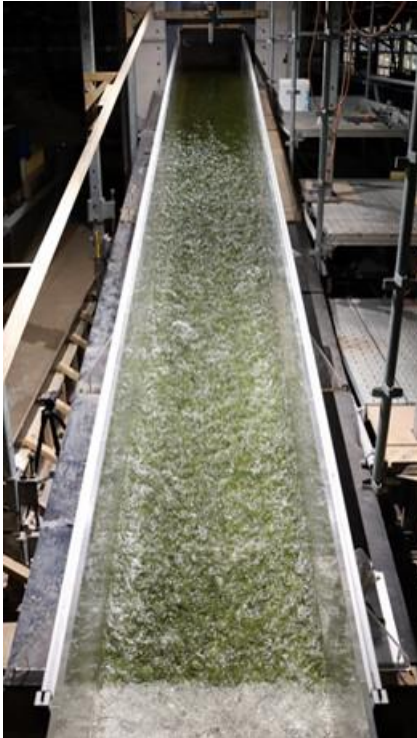
Artificial turf

Concrete Mat

0.06



0.125

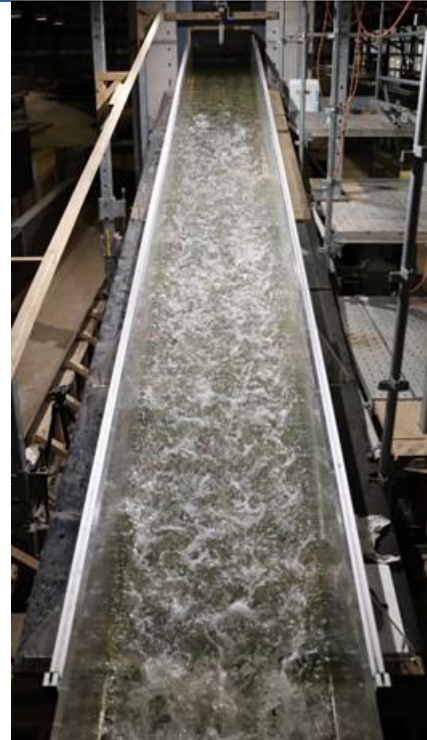


q (m³/s/m)

Artificial turf

Concrete Mat

0.188



0.250

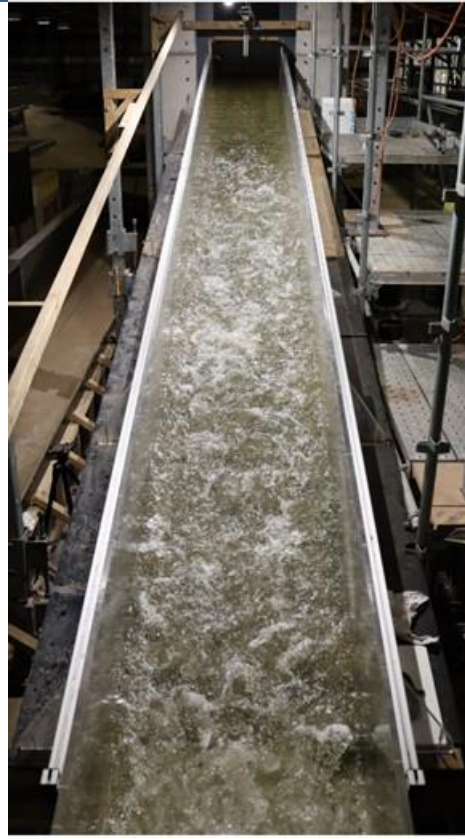


q (m³/s/m)

Artificial turf

Concrete Mat

0.313



0.375

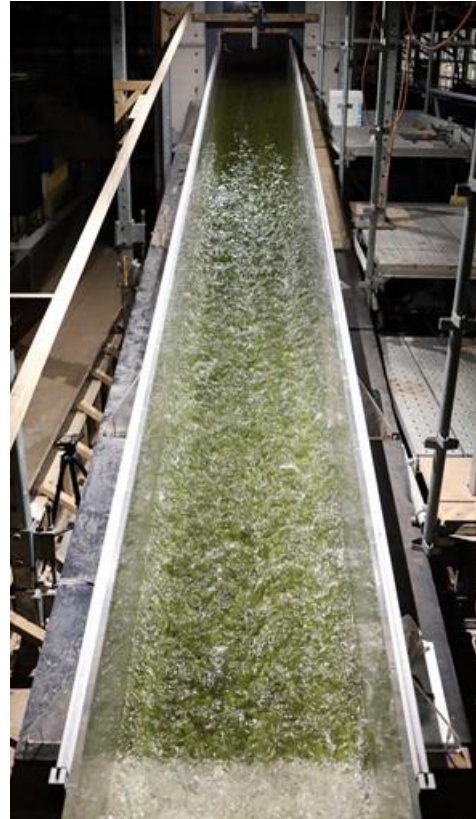






Table 3-3 Aeration comparison for tests conducted with and without the concrete mat

q ($m^3/s/m$)	Artificial turf	Concrete Mat
0.03		
0.06		

q
(m³/s/m)

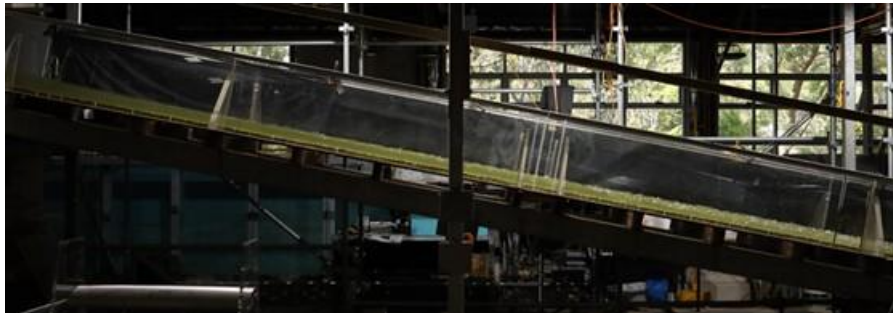
Artificial turf

Concrete Mat

0.125



0.188



0.250



q
(m³/s/m)

Artificial turf

Concrete Mat

0.313



0.375



4 Measurements

This section summarises the measurements and hydraulic calculations.

As discussed in Section 3, a major difference between the artificial turf tests and the concrete mat tests was the aeration of the flow. For artificial turf tests, the flow depths could be measured directly at the water surface by the ultrasonic sensors, i.e. water surface recorded with the ultrasonic is equal to the clear-water flow depth. For the aerated concrete mat tests, the flow depth is the sum of the air bubbles and water, and therefore, the flow depth recorded with the ultrasonic is different to the equivalent clear water flow depth. The equivalent clear-water flow depth was calculated using a method which has been found in previous studies to best represent the flow depth in aerated flows (Wood, 1991). The method is discussed in detail in Appendix A2.

4.1 Flow depth

Figure 4-1 presents the representation of the flow depths for the artificial turf experiment. In this case, the flow depth was considered as the distance from the top of the bend grass height and the free-surface measured with the ultrasonic.

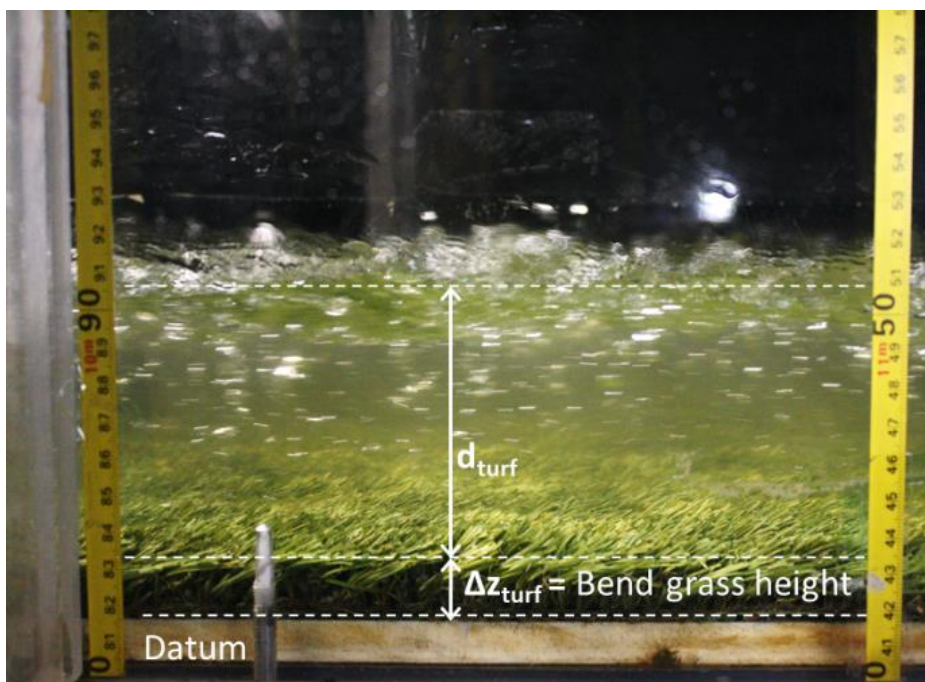


Figure 4-1 Definition of artificial turf flow depth elevation

For the concrete mattress test, the flow depth was considered as the distance from the bottom of the geotextile (in the intersection between the blocks) to the free-surface measured with the conductivity probe (d_{mattress}) (Figure 4-2). This flow depth represents the most critical scenario since most of the dissipation process was generated on top of the blocks and not within the intersection between the blocks.

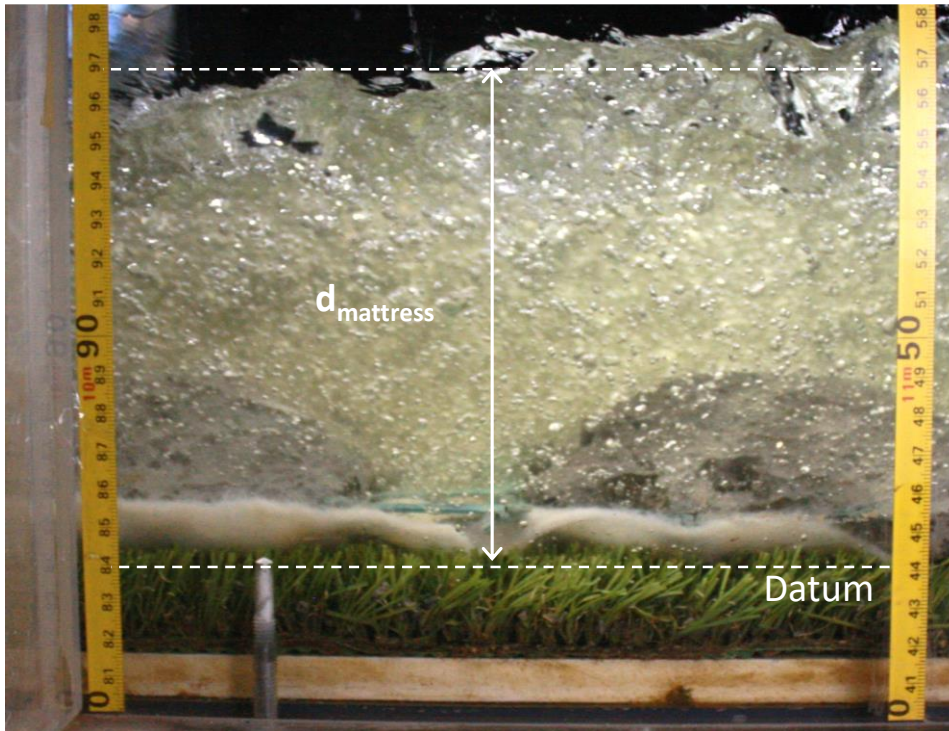


Figure 4-2 Definition of concrete flow depth elevations

Figure 4-3 presents the uniform flow depths ($d_{mattress}$ and d_{turf}) for various flows. Differences in the flow depth comparison are summarised below:

- In agreement with the visual observations, higher flow depths were recorded for the tests conducted with the concrete mattress with flow depth increases of more than 1.5 times d_{turf} . The increase in the flow depth is linked with the entrained air and the macroroughness.
- Major differences were identified in the flow depth between the tests conducted with the concrete mattress in the channel centre-line and channel side-line for flows lower than $0.06 \text{ m}^3/\text{s}/\text{m}$. These differences were linked with the generation of hydraulic jumps above the concrete blocks (channel side-line measurements) while channelised flows with lower flow depths and faster velocities were recorded in the channel centre-line.
- For flows larger than $0.06 \text{ m}^3/\text{s}/\text{m}$, the flow depths were similar for measurements undertaken in the channel centre-line and side-line of the concrete mat.

Note that the flow depth was taken as the temporal average of the most downstream cross section. Checks were made to ensure that uniform flow depth had been achieved (Appendix B).

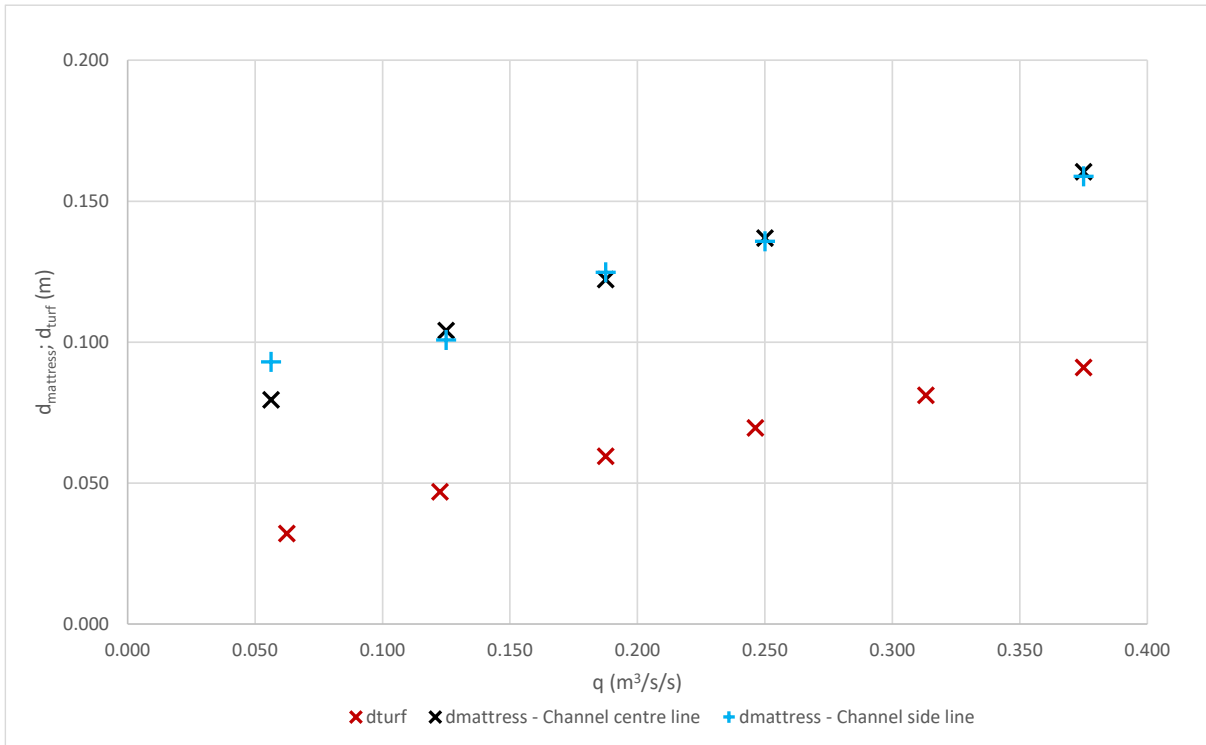


Figure 4-3 Comparison uniform flow depths

4.2 Depth averaged velocity

The averaged flow velocity was estimated based on the discharge and the clear-water flow depth as:

$$V = q/d \quad \text{Equation 3}$$

Figure 4-4 presents the comparison of the averaged flow velocity and the critical velocity (V_c) as a function of q . The critical velocity was calculated based on the critical flow depth d_c , where d_c was estimated as $d_c = (q^2/g)^{1/3}$ (only valid for rectangular channels) and g is the gravitational acceleration. Differences in the mean flow velocity were observed between the tests conducted with the artificial turf and the concrete mat:

- Independent of the channel bed roughness, the velocity increased with increasing discharge with a steeper increase for flows lower or equal to $0.2 \text{ m}^3/\text{s}/\text{m}$.
- The tests conducted with the concrete mattress showed a decrease in the mean flow velocity compared with the tests conducted with the artificial turf.
- Despite some data scatter, the concrete mattress caused a flow velocity reduction of about 30% for the lower flows and 60% for the larger flows compared with the tests conducted with the artificial turf.
- Subcritical flow conditions were observed for concrete mat flows of $0.06 \text{ m}^3/\text{s}/\text{m}$ suggesting slow flow conditions and low erosion risk for the intermediate region between the concrete blocks.

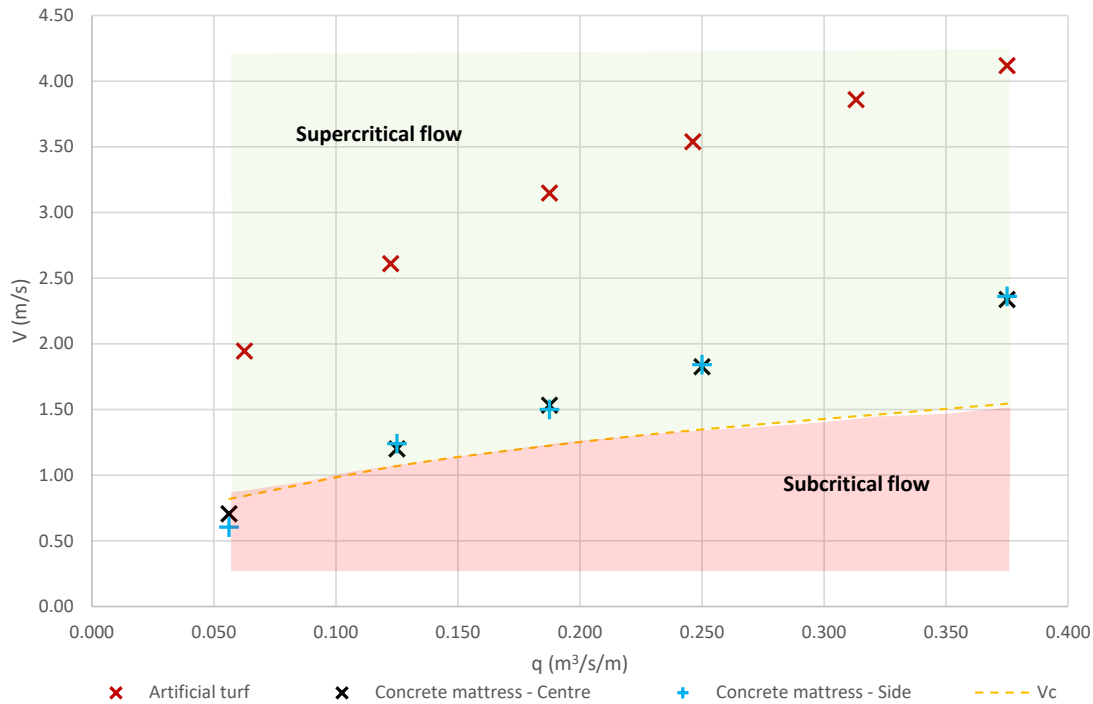


Figure 4-4 Comparison of mean velocity considering discharges without and with concrete mattress

4.3 Shear stress

The mean shear stress represents the friction generated by the roughness of the channel bed. The shear stress is estimated based on Equation 4.

$$\tau_0 = \rho \times g \times R_h \times S_0 \tag{Equation 4}$$

where T_0 is the mean shear stress

ρ is the water density

R_h is the hydraulic radius defined as $R_h = A/P$, A is the wetted area and P the wetted perimeter. For this study, $R_h = d$ since the tests were conducted in a wide channel ($b/d \geq 4$)

S_0 is the channel bed slope since the flow was uniform

Figure 4-5 presents the comparison between the shear stress as function of the discharge. Observations include:

- For all conditions, the mean shear stress in the channel bed increased with increasing q .
- Larger shear stress was identified for the concrete mattress condition highlighting higher flow reduction in this condition.
- Overall, the shear stress increase of the concrete mat tests was more than twice the shear stress in the artificial turf for the lower flows and more than 50% for the larger flows, which was linked with the larger submergence of the macro-roughness for deeper flow depths.

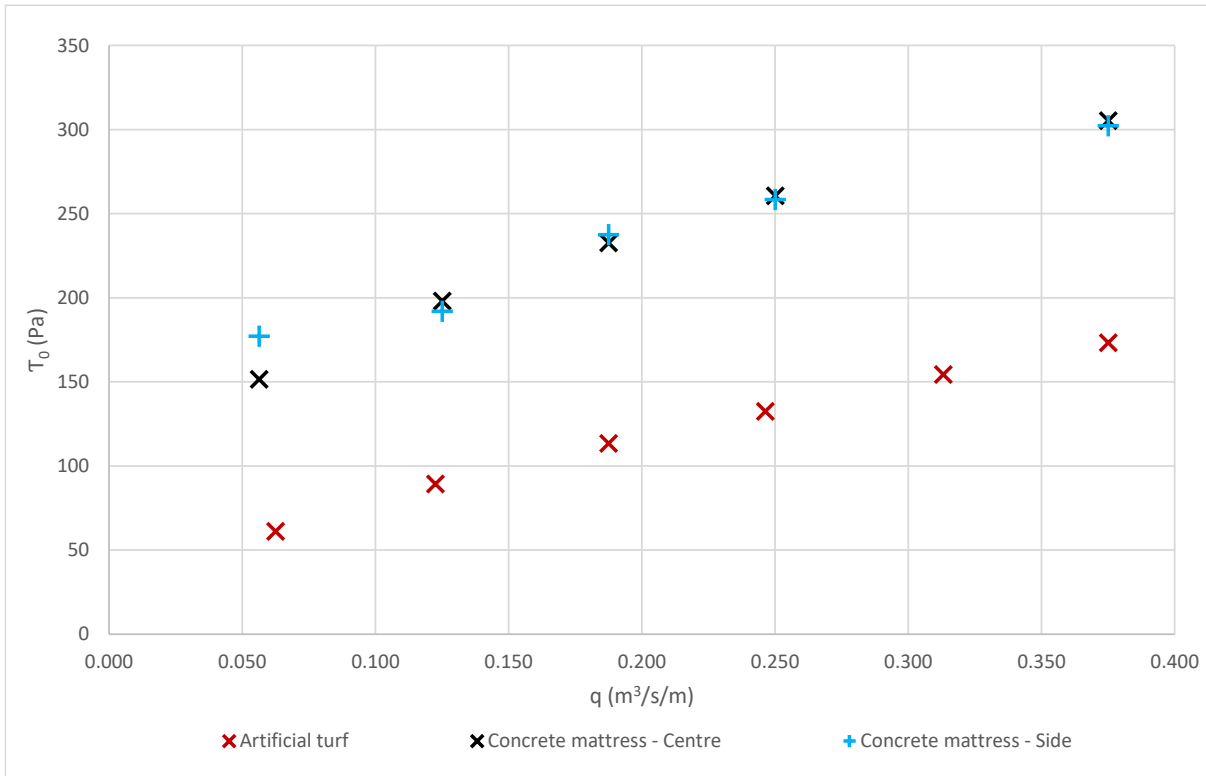


Figure 4-5 Comparison of mean shear stress considering discharges without and with concrete mattress

4.4 Darcy friction factor

The Darcy friction factor f represents the friction losses due to the roughness of the channel bed and the hydraulic parameters. The friction factor is estimated based on Equation 5:

$$f = \frac{8 \times g \times S_0 \times (R_h)}{V^2} \quad \text{Equation 5}$$

where

S_0 is the slope of the channel

R_h is the hydraulic radius.

Note that the friction factor was estimated based on S_0 since the flow conditions were uniform where measurements were taken. Figure 4-6 presents the Darcy friction factors for the artificial turf and the concrete mat tests. Observations include:

- For all the tests, the flow was completely turbulent.
- Large differences in the friction factor were identified for flows of $0.06 \text{ m}^3/\text{s}/\text{m}$ where the friction factor of the concrete mat was more than ten (10) times the friction factor estimated in the artificial turf.
- For flows larger than $0.125 \text{ m}^3/\text{s}/\text{m}$, the friction factor of the concrete mat was more than five (5) times the friction factor for the artificial turf.

- A slight decrease in the difference between the friction factor of the concrete mat and the artificial turf was identified for the largest flow, which was linked to the lesser macro-roughness effect in deeper water depths.
- Figure 4-6 also shows that the friction factor is a function of the discharge. Larger friction factors were identified for lower discharges where the macro-roughness is significantly affecting the surface roughness. For larger discharges, the friction factor decreased with increasing the discharge at a smaller rate, compared with the decrease in the lower discharges since the roughness is less representative compared to the flow depth.

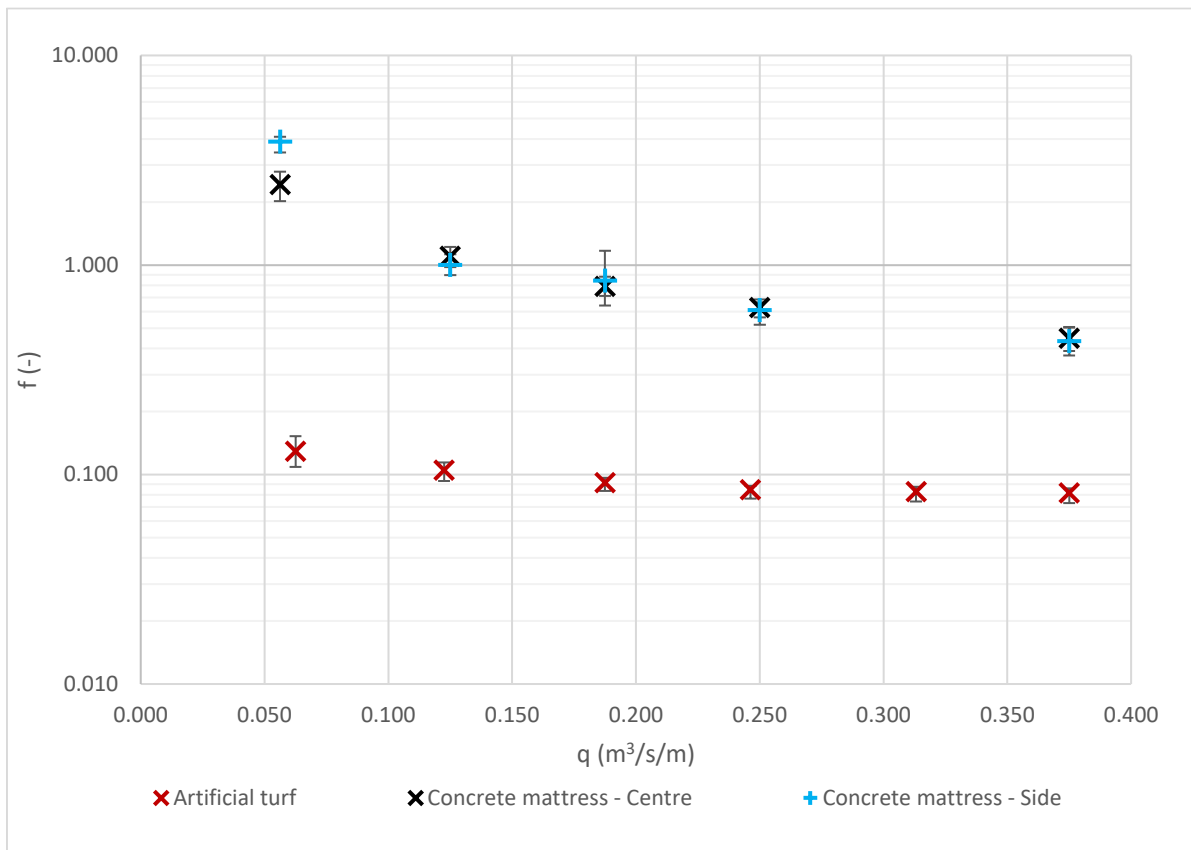


Figure 4-6 Comparison of Darcy friction factors

Figure 4-7 presents the Darcy friction factor as a function of the time-averaged flow depth for the concrete mattress condition. The friction factor decreased with increasing the flow depth suggesting lesser effect of the macro-roughness for deeper flow depths. For the present tests, the flow depths varied from 0.08 m to 0.16 m resulting in friction factors between 0.4 to 2.4. The wide range in the friction factor highlighted the strong variation of the friction factor values with the discharge which is expected in macro-rough conditions.

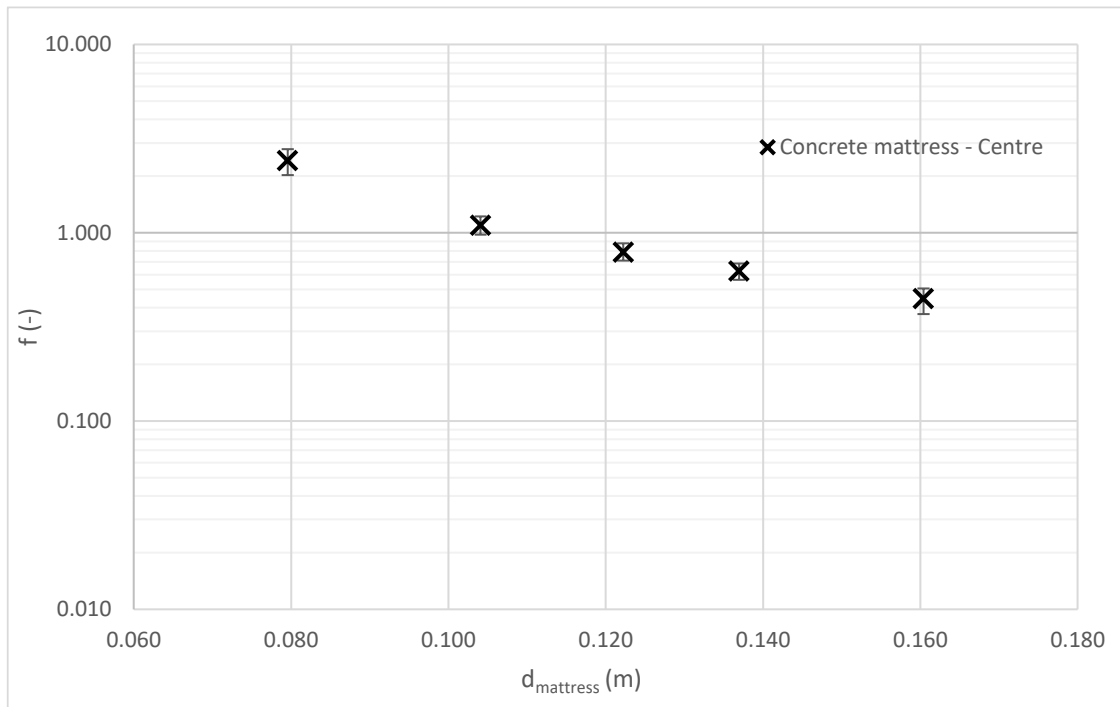


Figure 4-7 Darcy friction factor as a function of the flow depth

4.5 Manning coefficient

Figure 4-8 presents the Manning's coefficient (n) for the concrete mat tested in the present study. Manning's coefficient was estimated based on the Darcy friction factor as:

$$n^2 = \frac{f \times R_h^{1/3}}{8 \times g} \quad \text{Equation 6}$$

The Manning's coefficient values registered in the present study for the concrete mats are between a typical range of Manning's n coefficients for natural channels and floodplains (Ball et al., 2019). Typically, the Darcy friction factor is preferred in the estimation of friction losses since the Manning's equation is not suggested for shallow flow depths.

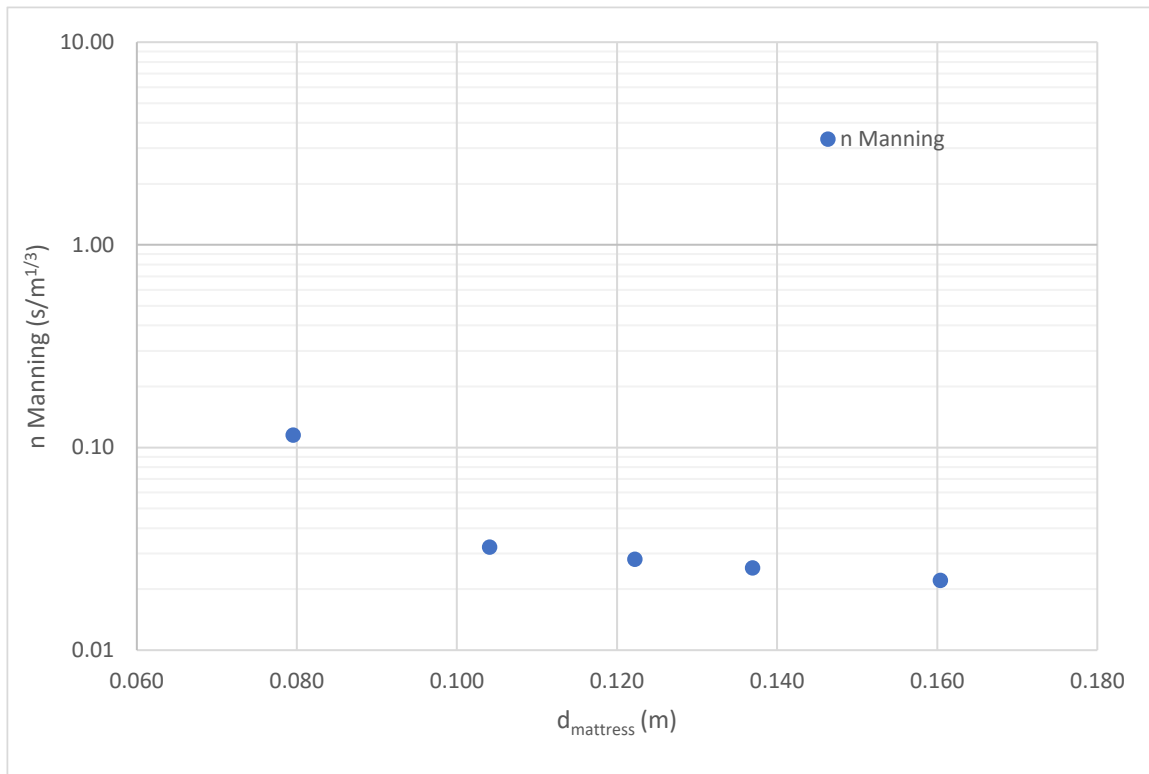


Figure 4-8 Manning's "n" coefficient for concrete mats

5 Example of calculating uniform flow depth and velocity for the concrete mats

The uniform flow depth of an open channel with an installed concrete mat of 58 mm height, and a block size area of 160 mm x 148 mm can be estimated using Figure 5-1.

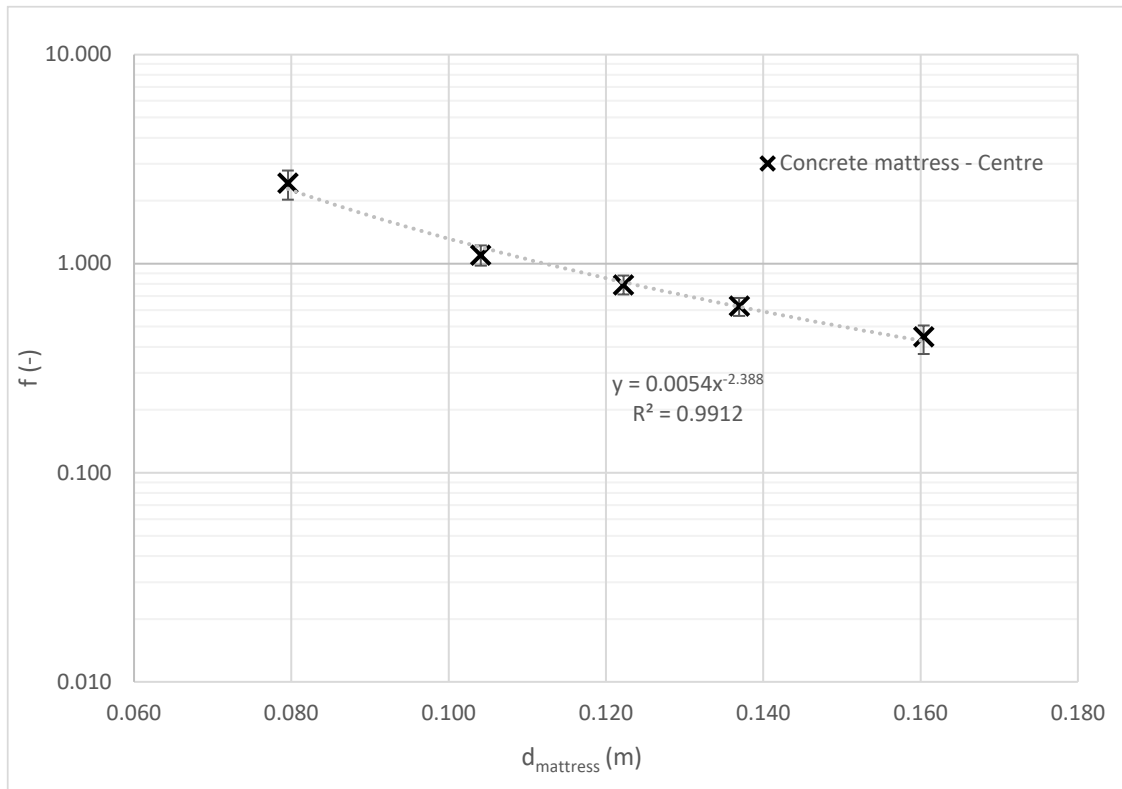


Figure 5-1 Darcy friction factor for the concrete mat as a function of the flow depth

An example for estimating the uniform flow depth is presented below:

1. Assume a total discharge of 300 L/s in a rectangular channel of width of 2 m and a slope of 0.1.

$$\begin{aligned} Q &= 300 \text{ L/s} \\ B &= 2 \text{ m} \\ S &= 0.1 \end{aligned}$$

2. Estimate the flow per unit of width (q)

$$q = \frac{Q}{B} = \frac{300 \text{ L/s}}{2 \text{ m}} = 0.15 \text{ m}^3/\text{s}$$

3. Guess an initial flow depth ($d_{i,0}$).

$$d_{i,0} = 0.12 \text{ m}$$

4. Identify f based on the equation presented in Figure 5-1

$$f_1 = 0.0054 \times d_{1,0}^{-2.388} = 0.0054 \times 0.12^{-2.388} = 0.854$$

5. Estimate mean flow velocity

$$V_1 = \frac{q}{d_{1,0}} = \frac{0.15 \text{ m}^3/\text{s}/\text{m}}{0.12 \text{ m}} = 1.25 \text{ m/s}$$

6. Estimate the flow depth rearranging Equation 1 ($d_{i,eq}$). Note that the equation below considered a wide rectangular channel and d was used instead of R_h .

$$d_{1,eq} = \frac{f \times V^2}{8 \times g \times S_0} = \frac{0.854 \times (1.25 \text{ m/s})^2}{8 \times (9.81 \text{ m/s}^2) \times 0.1} = 0.17 \text{ m}$$

7. Compare $d_{1,0}$ and $d_{1,eq}$

$$\begin{aligned} d_{1,0} &= 0.12 \text{ m} \\ d_{1,eq} &= 0.17 \text{ m} \\ d_{1,eq} - d_{1,0} &= +0.08 \text{ m} > 0.005 \text{ m} \end{aligned}$$

8. Since $|d_{1,eq} - d_{1,0}| > 0.005 \text{ m}$, you need to iterate again. If $d_{1,eq} - d_{1,0} > 0.005$, $d_{2,0}$ should be larger than $d_{1,0}$.

$$d_{2,0} = 0.131 \text{ m}$$

9. Recalculate f for the new flow depth $d_{2,0}$

$$f_2 = 0.0054 \times 0.131^{-2.388} = 0.69$$

10. Recalculate mean flow velocity for the new flow depth

$$V_2 = \frac{0.15 \text{ m}^3/\text{s}/\text{m}}{0.131 \text{ m}} = 1.14 \text{ m/s}$$

11. Recalculate the flow depth rearranging Equation 1 ($d_{i,eq}$).

$$d_{2,eq} = \frac{0.69 \times (1.14 \text{ m/s})^2}{8 \times (9.81 \text{ m/s}^2) \times 0.1} = 0.131 \text{ m}$$

12. Compare $d_{1,0}$ and $d_{1,eq}$

$$\begin{aligned} d_{2,0} &= 0.131 \text{ m} \\ d_{2,eq} &= 0.131 \text{ m} \\ d_{2,eq} - d_{2,0} &= 0.00 \text{ m} < 0.005 \text{ m} \end{aligned}$$

13. Since $d_{2,eq} - d_{2,0} < 0.005 \text{ m}$, the uniform flow depth of a 2 m wide rectangular channel, for a discharge of 300 L/s and a slope of 0.1 is **0.131 m**.

Figure 5-2 presents a flow chart with the methodology for estimating the uniform flow depth and mean flow velocities for open channels with concrete mats.

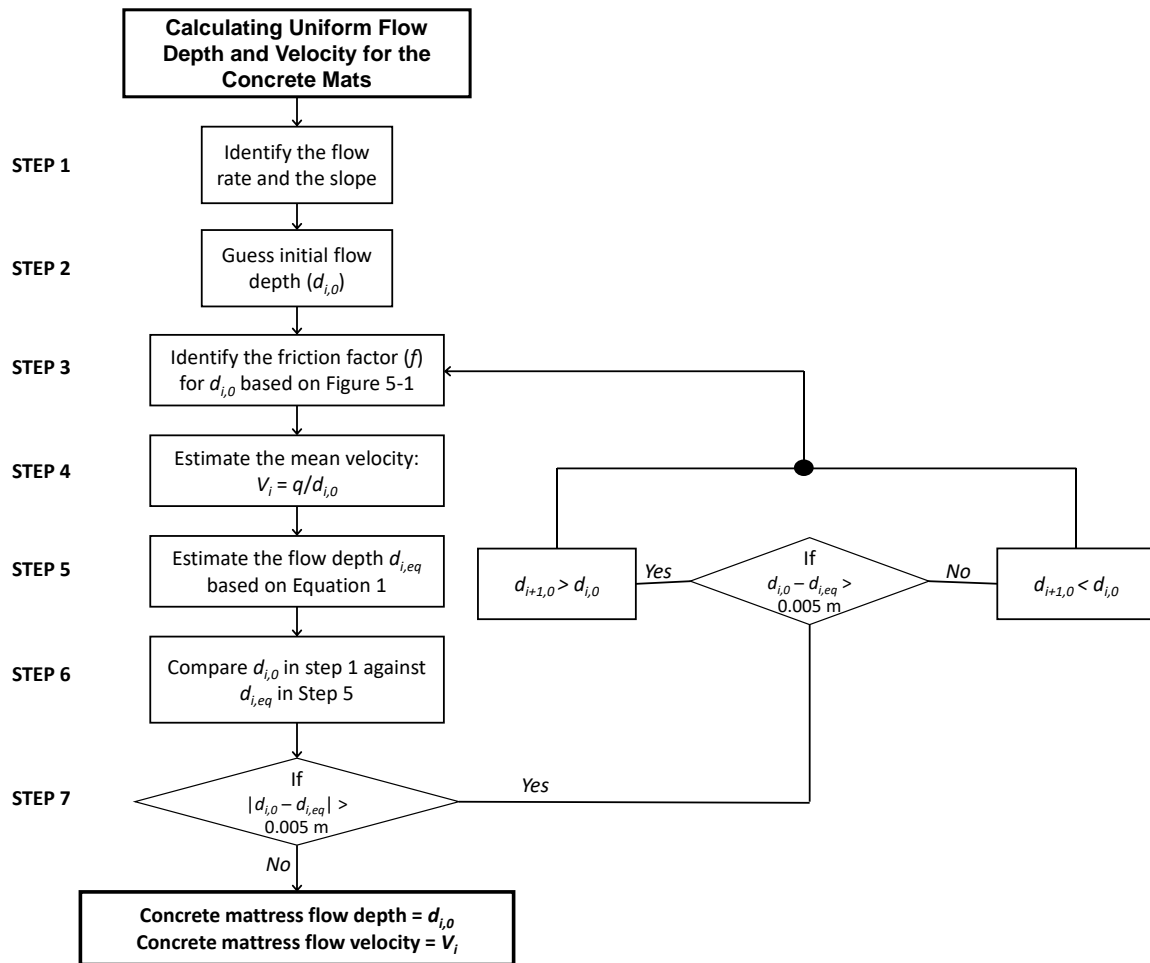


Figure 5-2 Flow chart for estimating uniform flow depths and mean flow velocities for open channels with concrete mats

6 References

- Ball, J, Babister M, Nathan, R, Weeks, W, Weinmann, E, Retallick, M & Testoni, I, (Editors) Australian Rainfall and Runoff: A Guide to Flood Estimation, © Commonwealth of Australia (Geoscience Australia), 2019. http://www.arr-software.org/pdfs/ARR_190514_Book6.pdf
- Cartellier, A and Achard, J L 1991, 'Local phase detection probes in fluid/fluid two-phase flows', *Review of Scientific Instruments*, vol. 62, no. 2, pp. 279-303.
- Chanson, H. and Toombes, L 2002, 'Air-water flows down stepped chutes: turbulence and flow structure observations', *International Journal of Multiphase Flow*, vol. 28, pp. 1737–1761.
- Felder, S 2013, 'Air-Water Flow Properties on Stepped Spillways for Embankment Dams: Aeration, Energy Dissipation and Turbulence on Uniform, Non-Uniform and Pooled Stepped Chutes', *Ph.D. Thesis*, School of Civil Engineering, The University of Queensland, Australia, 506 pages.
- Felder, S and Pfister, M 2017, 'Comparative analyses of phase-detective intrusive probes in high-velocity air-water flows', *International Journal of Multiphase Flow*, vol. 90, pp. 88-101.
- Felder, S and Chanson, H 2015, 'Phase-detection probe measurements in high-velocity free-surface flows including a discussion of key sampling parameters'. *Experimental Thermal and Fluid Science*, vol. 61, pp. 66-78.
- Landcom, 2004 *Managing Urban Stormwater: Soils and Construction*, Volume 1, Fourth Edition, NSW Government, Parramatta, NSW.
- Scheres, B, Schüttrumpf, H and Felder S. 2019, 'Flow Resistance and Energy Dissipation in Supercritical Air-Water Flows Down Vegetated Chutes', *Water Resources Research*, vol. 56.
- Toombes, L. 2002, 'Experimental study of Air-Water Flow Properties on Low-Gradient Stepped Cascades', *Ph.D. Thesis*, Dept. of Civil Engineering, The University of Queensland, Australia, 304 pages.
- Wood, I R 1991, 'Air Entrainment in Free-surface Flows', *IAHR Hydraulic Structures Design Manual No. 4*, Hydraulic Design Considerations, Balkema Publ, Rotterdam, The Netherlands, p.149.
- Zhang, G., Valero, D., Bung, DB., and Chanson, H. 2018, 'On the estimation of free-surface turbulence using ultrasonic sensors', *Flow Measurement and Instrumentation*, vol. 60, pp. 171–184.

Appendix A Instrumentation

A1 Flow rates

The flow rates were achieved with a Brook Crompton, 3 phase motor pump and measured using an ABB® electromagnetic flowmeter with an accuracy of $\pm 0.4\%$.



Figure A-1 Brook Crompton centrifugal pump

A2 Flow depths

A2.1 Ultrasonics:

For all conditions (artificial turf and concrete mat tests), the flow depths were recorded simultaneously with four ultrasonic water level sensors located every 0.25 m between 7 m and 7.75 m. The ultrasonics were installed in a wood frame. Each ultrasonic was calibrated before starting the experiments.



Figure A-2 Ultrasonic arrangement in the channel centre line

The flow depth was estimated as the time-average flow depth recorded during 3 minutes. Since some water droplets reached the ultrasonic sensors for the large flow conditions, a minimum and maximum threshold was selected for each flow condition. In addition, following the approach of Zhang et al. (2018), any flow depth larger or lower than 3 times the standard deviation of the complete data recording was also filtered.

A2.2 Double-tip conductivity probe:

Since the experiments conducted with the concrete mattress showed larger flow aeration, the free-surface profile was also recorded with a double-tip conductivity probe at four different cross-sections and several elevations in the channel centre line and on the channel side. Double-tip conductivity probes have been widely used in the analysis of aerated flows comprising flows in spillways, tunnels and hydraulic jumps (Chanson and Toombes 2002; Felder and Pfister 2017). In the present study, the conductivity probe had a longitudinal separation distance of $\Delta x = 5.71$ mm and transversal separation distance of $\Delta z = 1.05$ mm. The time-averaged air concentration with the conductivity probe was estimated based on the single threshold technique where any value larger than 50% of the difference between the peaks of the bimodal distribution of the raw voltage signal is considered as water and values lower than 50% are considered as air (Cartellier and Achard 1991; Toombes 2002; Felder 2013; Felder and Chanson 2015).

For the experiments conducted with the concrete mat, the flow depth elevation ($d_{mattress}$) measured with the conductivity probe was estimated based on the equivalent clear-water flow depth for aerated flows which is calculated based on the air concentration distribution (Equation 5):

$$d_{90} = \int_{y=0}^{y=Y_{90}} (1 - C) \times dy \quad \text{Equation A-1}$$

where d_{90} represents the equivalent clear-water flow depth with an upper integration limit of Y_{90} , y is the vertical position above the datum, Y_{90} is the characteristic depth where the air concentration is 90% and C is the air concentration.

Appendix B Uniform flow conditions

The flow depth measurements were undertaken at the end of the sloped channel aiming to obtain uniform flow conditions. Figure B-1 presents the flow depth measured with the conductivity probe – CP (solid symbols) and the ultrasonics – US (hollow symbols) as function of the four different cross-sections measured along the channel. Despite some data scatter, the flow depths recorded with each instrument were similar along the different cross-sections with average differences of ± 5 mm for the concrete mattress experiments and ± 2 mm for the artificial turf experiments, suggesting similarity at different locations and therefore, uniformity. Overall, flow depths measured with the ultrasonic sensor were approximately 5% higher compared with the clear-water flow depth measured with the conductivity probe.

The uniformity for air-water flows was also estimated based on the mean air concentration. The mean air concentration was estimated based on Equation 6:

$$C_{mean} = \frac{1}{Y_{90}} \int_{y=0}^{y=Y_{90}} C \times dy \tag{Equation B-1}$$

where C_{mean} is the mean air concentration. Independent of the flow condition, the mean air concentration was similar for the four cross-sections investigated in the present study with maximum differences of 3% for the channel centre line measurements. This insight validated uniform flow conditions at the downstream end of the spillway flume.

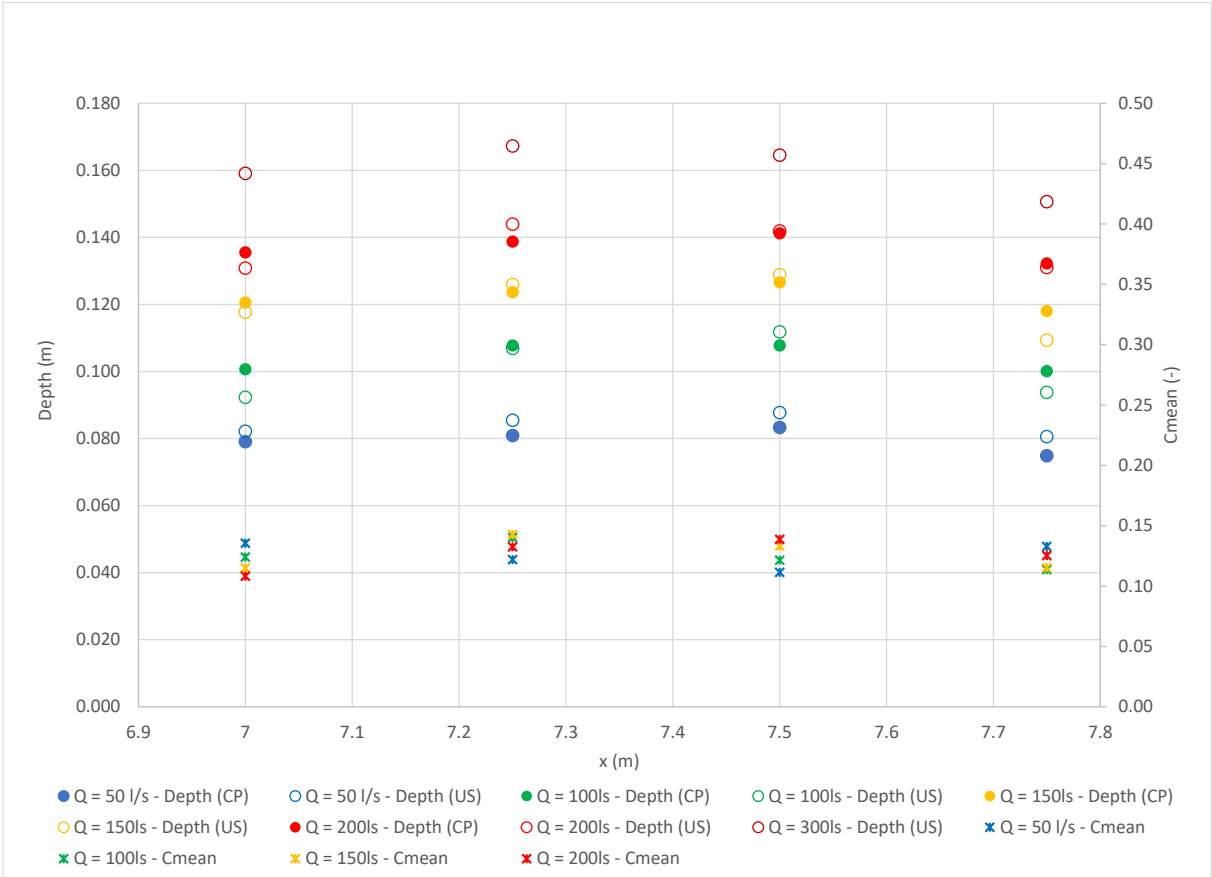


Figure B-1 Uniform flow conditions in channel centre line at the downstream end of the flume